NASA/TP—2002-211108

COSP for Windows: Strategies for Rapid Analyses of Cyclic Oxidation Behavior

James L. Smialek and Judith V. Auping
Glenn Research Center, Cleveland, Ohio

February 2002

The NASA STI Program Office . . . in Profile

Since its founding, NASA has been dedicated to the advancement of aeronautics and space science. The NASA Scientific and Technical Information (STI) Program Office plays a key part in helping NASA maintain this important role.

The NASA STI Program Office is operated by Langley Research Center, the Lead Center for NASA's scientific and technical information. The NASA STI Program Office provides access to the NASA STI Database, the largest collection of aeronautical and space science STI in the world. The Program Office is also NASA's institutional mechanism for disseminating the results of its research and development activities. These results are published by NASA in the NASA STI Report Series, which includes the following report types:

- TECHNICAL PUBLICATION. Reports of completed research or a major significant phase of research that present the results of NASA programs and include extensive data or theoretical analysis. Includes compilations of significant scientific and technical data and information deemed to be of continuing reference value. NASA's counterpart of peer-reviewed formal professional papers but has less stringent limitations on manuscript length and extent of graphic presentations.

- TECHNICAL MEMORANDUM. Scientific and technical findings that are preliminary or of specialized interest, e.g., quick release reports, working papers, and bibliographies that contain minimal annotation. Does not contain extensive analysis.

- CONTRACTOR REPORT. Scientific and technical findings by NASA-sponsored contractors and grantees.

- CONFERENCE PUBLICATION. Collected papers from scientific and technical conferences, symposia, seminars, or other meetings sponsored or cosponsored by NASA.

- SPECIAL PUBLICATION. Scientific, technical, or historical information from NASA programs, projects, and missions, often concerned with subjects having substantial public interest.

- TECHNICAL TRANSLATION. English-language translations of foreign scientific and technical material pertinent to NASA's mission.

Specialized services that complement the STI Program Office's diverse offerings include creating custom thesauri, building customized data bases, organizing and publishing research results . . . even providing videos.

For more information about the NASA STI Program Office, see the following:

- Access the NASA STI Program Home Page at *http://www.sti.nasa.gov*

- E-mail your question via the Internet to help@sti.nasa.gov

- Fax your question to the NASA Access Help Desk at 301–621–0134

- Telephone the NASA Access Help Desk at 301–621–0390

- Write to:
  NASA Access Help Desk
  NASA Center for AeroSpace Information
  7121 Standard Drive
  Hanover, MD 21076

NASA/TP—2002-211108

COSP for Windows: Strategies for Rapid Analyses of Cyclic Oxidation Behavior

James L. Smialek and Judith V. Auping
Glenn Research Center, Cleveland, Ohio

National Aeronautics and
Space Administration

Glenn Research Center

February 2002

Trade names or manufacturers' names are used in this report for identification only. This usage does not constitute an official endorsement, either expressed or implied, by the National Aeronautics and Space Administration.

Available from

NASA Center for Aerospace Information
7121 Standard Drive
Hanover, MD 21076

National Technical Information Service
5285 Port Royal Road
Springfield, VA 22100

Available electronically at http://gltrs.grc.nasa.gov/GLTRS

COSP for Windows: Strategies for Rapid Analyses of Cyclic Oxidation Behavior

James L. Smialek and Judith V. Auping
National Aeronautics and Space Administration
Glenn Research Center
Cleveland, Ohio 44135

Summary

COSP is a publicly available computer program that models the cyclic oxidation weight gain and spallation process. Inputs to the model include the selection of an oxidation growth law and a spalling geometry, plus oxide phase, growth rate, spall constant, and cycle duration parameters. Output includes weight change, the amounts of retained and spalled oxide, the total oxygen and metal consumed, and the terminal rates of weight loss and metal consumption. The present version is Windows based and can accordingly be operated conveniently while other applications remain open for importing experimental weight change data, storing model output data, or plotting model curves. Point-and-click operating features include multiple drop-down menus for input parameters, data importing, and quick, on-screen plots showing one selection of the six output parameters for up to 10 models. A run summary text lists various characteristic parameters that are helpful in describing cyclic behavior, such as the maximum weight change, the number of cycles to reach the maximum weight gain or zero weight change, the ratio of these, and the final rate of weight loss. The program includes save and print options as well as a help file. Families of model curves readily show the sensitivity to various input parameters. The cyclic behaviors of nickel aluminide (NiAl) and a complex superalloy are shown to be properly fitted by model curves. However, caution is always advised regarding the uniqueness claimed for any specific set of input parameters.

Introduction: Model Overview

COSP for Windows (WinCOSP is the abbreviated program file name) is an adaptation of original cyclic oxidation models developed at NASA Glenn Research Center over a period of 25 years (refs. 1 to 8). Some papers documenting many of the precepts and findings are listed in these references and related bibliographies (refs. 9 to 15). Original mainframe versions were written in Fortran, and later a version for personal computers was written in Modula-2 and described in a complete archival treatise (ref. 7). It is hoped that this Windows version will further increase its user-friendly attributes and broaden its base of users.

Basically, the program calculates a cyclic oxidation weight change curve by using some elementary inputs and assumptions regarding model scale growth and spalling behavior. Along with the sample weight change, other factors germane to the cyclic process—oxygen consumed, metal consumed, scale weight, spall weight—are all part of the calculations. Key descriptive parameters, such as number of cycles to maximum weight gain, cycles to cross zero weight change, final weight loss slope, and the plateau in oxygen gain, are all highlighted as part of the text output.

The mechanics of the calculation are briefly described by way of introduction. A type of oxide is chosen (e.g., alumina, Al_2O_3) in order to determine a stoichiometric constant S_c, or the weight ratio of oxide to oxygen in the scale. This constant relates the amount of oxide weight (metal + oxygen) to that of oxygen in the scale (e.g., 2.124 for Al_2O_3). A growth model may be chosen, but typically parabolic rates are assumed, where the specific weight change $\Delta W/A$ is given by equation (1). Options for power law (eq. (2)) and logarithmic growth (eq. (3)) are also included:

$$(\Delta W/A)^2 = k_p t \tag{1}$$

$$(\Delta W/A)^m = kt \tag{2}$$

$$\Delta W/A = \ln\left[(kt + c)^{1/m}\right] \tag{3}$$

where k_p is the parabolic rate constant, k is the growth rate for the other models, t is time, c is a secondary growth constant, and m is a growth exponent.

The growth model is used to calculate the amount of scale grown at temperature during one cycle. The amount of spallation that occurs during the cooling portion of the cycle is governed by the spall constant Q_0. The fraction spalled F_s of the existing scale weight W_r' is given by

$$F_s = (Q_0)(W_r')^{\alpha} \tag{4}$$

where α is the spall exponent, a constant usually assumed to be 1.0 (as found in some independent tests of spall amount versus scale weight, refs. 2, 4, and 7). It is important to note that Q_0 is not strictly a spall fraction or percentage. The remaining amount of oxide after C cycles $W_{r,C}$ and the effective time $t_{\text{eff},C}$ that corresponds to the isothermal growth of this amount of oxide are then calculated. The scale present during the next heating cycle $W'_{r,C+1}$ can then be determined on the basis of the growth model, but now by using the time $t_{\text{eff}} + \Delta t$, where Δt is simply the cycle duration. This sequence of calculations is seen by inspection of equations (5) to (7) below. Repetition of these calculations for a preset number of cycles generates the scale weight and allows calculation of the entire cyclic oxidation curve.

$$W_r = W'_r - F_s W'_r \tag{5}$$

$$W'_{r,C} = S_c\left(k_p \Delta t\right)^{1/2} \tag{6}$$

$$W'_{r,C+1} = S_c\left[k_p\left(t_{\text{eff},C} + \Delta t\right)\right]^{1/2} \tag{7}$$

In addition to Q_0 as an input for spalling, the spallation "geometry" must also be specified. The spallation geometry describes whether the material is removed as a uniform layer off the top of the entire scale or whether it is removed in discrete areas as "chunks" of specified thickness. For many instances the uniform spalling layer provides a reasonable approximation of the average behavior of systems that do not exhibit primarily interfacial spallation. Nonuniform or discrete spallation areas are more precisely handled by the Monte Carlo bimodal calculations. Within this option the sample surface is divided into a specified number of equivalent segments. The total spall fraction F_s is given by $F_{\text{avg}} = P(R_{\text{spall}})$, where P is the probability and R_{spall} is the depth fraction (specified from the input menu) of the spalled segment for a bimodal distribution of spall geometry. A random number generator (0 to 1.0) is used to provide a random value RN for each segment, and when (RN) < P, that segment is tagged for spallation of the fractional depth R_{spall} on that cycle. The total spall fraction of the scale is summed over all the segments and is equal to $F_{\text{avg}} = Q_0 (W'_r)^{\alpha}$. The specific scale measures for each segment are then cataloged and updated each cycle for the entire oxidation curve.

One final option is to use a rectangular distribution of spall probability (ref. 7), but in practice it is found to be indistinguishable from the uniform spalling case. The Windows program also allows for importing tables of experimental specific weight change versus time data, so that model curves can be directly compared with experimental results.

This report reviews the overall findings of the original COSP model as presented previously in references 3 to 8, with reference 7 offering the most complete development of the theory and critical analysis of the model results. These findings are presented in the format of what the COSP for Windows user experiences in stepping through the main windows and model options. Finally, having established that background, a few examples are given that show how the models can be used to fit the behavior of well-known, high-temperature, oxidation-resistant materials.

Basic Operating Features

COSP for Windows requires Windows95 or later versions. Three windows are always accessible by large point-and-click buttons: the **Plot window**, the **Results window**, and the **Experimental data** window, whose major features are described below. (The specific window titles, menu lists, and buttons are displayed here in boldface type.)

Plot Window

Under the **Plot window**, the **Setup** dialog window is used to define the model parameters and plot the curves. It appears when the program is started, using the initialization default parameters (Al_2O_3, k_p = 0.01 mg^2/cm^{4}hr; uniform spall with Q_0 = 0.01, α = 1, and Δt = 1 hr). The basic inputs are listed below:

1. **Oxide (Stoichiometric constant),** S_c
2. **Growth law:** parabolic, power law, or logarithmic
   a. Parabolic: (Specific weight gain)^2 = $k_p t$
   b. Power law: (Specific weight gain)^m = kt
   c. Logarithmic: Specific weight gain = $\ln[(kt + c)^{1/m}]$
   Rate constants, k_p (mg^2/cm^{4}hr) or k
   Growth exponent, m
   Secondary growth constant, c
3. Spall constant, Q_0
4. Spall exponent, α
5. **Spall case:**
   a. Uniform: $F_s = (Q_0)(W'_r)^{\alpha}$
   b. Monte Carlo: Bimodal F_{avg} assigned from
   $F_{\text{avg}} = (Q_0)(W'_r)^{\alpha} = P(R_{\text{spall}})$.
   Segment spalls if $P^* < P$, where P^* is assigned by a random number generator for each segment.
6. **Number of segments**
7. **Number of cycles,** C
8. **Time per cycle,** Δt, hr

An instant plot is shown in the graphic display field when the **Okay** button is clicked. The **Add another model** button allows the user to simultaneously display the results for up to 10 different models. Different model outputs for the y axis may be selected (e.g., **Cumulative oxygen uptake, Cumulative weight of metal consumed, Fraction of oxide spalled, Weight of retained oxide**, etc.) or, for the x axis, **Time (in hours)** or

Cycles. The resulting plot may be printed directly to any Windows-compatible printer. A short input listing will be printed for each existing model. The model parameters may be saved directly in a COSP for Windows folder for easy retrieval and future use in the program.

Results Window

A tabular display of all the calculated output data for the last model selected is presented in the **Results window**, as is a text summary of the input parameters and a description of the curve (see output list below). They may both be copied and pasted into spreadsheet or text applications. The **model** menu allows one to select and display the data for other models or to delete all the current models. The outputs are as follows:

1. Summary (text):
   a. Cycles to maximum weight change, C_m
   b. Maximum weight change, $(\Delta W/A)_{max}$
   c. Cycles to zero weight change, C_0
   d. Ratio C_m/C_0, or inverse
   e. Final slope (negative weight loss rate)
   f. Final metal consumption rate
   g. Final effective time, t_{eff}

2. Spreadsheet (table):
   a. Cumulative weights for
      Oxygen uptake
      Metal consumed
      Spalled oxide
   b. Weight of retained scale
   c. Fraction of oxide spalled, F_s
   d. Net weight change, $\Delta W/A$
   e. Effective time, t_{eff}

Experimental Data Window

Sets of experimental weight change data may also be imported by using a **Paste from clipboard** command in the **Experimental data window**. These data will be then plotted in the **Plot window**. This feature can be used to directly compare experimental oxidation curves with the results from the calculated models. The total number of experimental and model curves cannot exceed 10.

General Model Trends

Baseline Behavior

In this section some basic trends in the cyclic oxidation curve are reexamined as a function of all the input parameters. A standard baseline for comparison is offered assuming an Al_2O_3 scale with a parabolic growth rate of 0.01 mg^2/cm^4hr (representative of 1200 °C growth), uniform layer spallation with a Q_0 of 0.002 cm^2/mg, a cycle duration of 1 hr, and a test length of 1000 cycles. Many of the outputs for this model are plotted against time (cycles) in figure 1. The cyclic sample weight change curve reaches a maximum weight gain of about 0.66 mg/cm^2 at 85 cycles and reaches a negative weight change at 279.2 hr with a ratio C_m/C_0 of 0.30. The final slope in $\Delta W/A$ (linear weight loss rate) is 0.0053 mg/cm^2hr. As this linear rate is approached, so too are the linear rates of oxygen (ΣO_2) and aluminum (ΣAl) consumption as well as that of total oxide spalled (ΣW_{spall}). (It is useful to note that the final slope of the weight change curve is equivalent to the final rate of metal consumed (ref. 7).) Figure 1(a) shows that the net weight change curve is equal to the total oxygen reacted less the

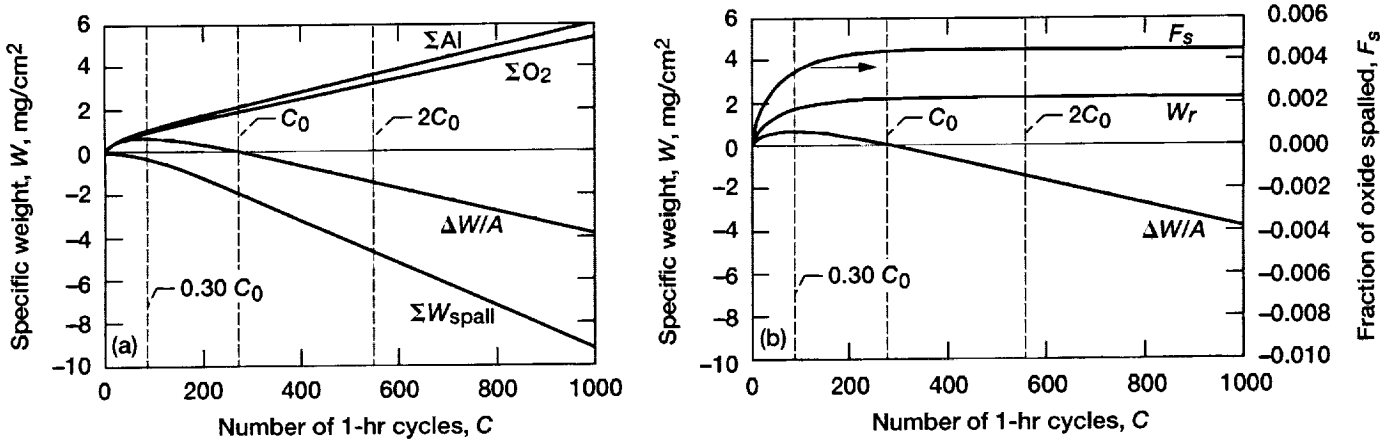

Figure 1.—Typical outputs from standard baseline COSP cyclic oxidation model. Parabolic growth and uniform spalling of Al_2O_3 scale with parabolic rate constant k_p, 0.01 mg^2/cm^4hr; spall constant Q_0, 0.002 cm^2/mg; and cycle duration Δt, 1 hr. (a) Net sample weight change $\Delta W/A$ related to total amount of oxygen (ΣO_2) and aluminum (ΣAl) consumed and amount of oxide spalled (ΣW_{spall}). (b) Net sample weight change related to existing scale weight W_r and scale fraction spalled F_s each cycle.

amount of oxide spalled ($\Sigma O_2 - \Sigma W_{spall}$). Figure 1(b) shows that the retained scale and consequently the fraction of scale spalled in each cycle approach a constant level at the same time that linear rates of weight loss, material consumed, and total oxide spalled are approached. These parameters achieve better than 92 percent of the final limits when the number of cycles $C = C_0$ and 99.9 percent of same when $C = 2C_0$. This steady-state behavior suggests that some extrapolation from relatively short-time testing is warranted from the model, provided that no mechanism changes take place.

Parametric Trends

The sets of weight change curves displayed in figures 2 to 6 represent major trends with the various input parameters. A baseline weight change curve (from fig. 1) is offered for comparison in each figure.

Stoichiometric constant.—In practice any variation in scale phase usually entails a consequential change in growth rate at any given temperature. However, for the purpose of showing the singular effect of varying the stoichiometry and composition of the scale alone, figure 2 displays a family of cyclic oxidation curves for alumina (Al_2O_3), chromia (Cr_2O_3), nickel aluminate spinel ($NiAl_2O_4$), nickel oxide (NiO), and nickel tantalate ($NiTa_2O_6$). It is apparent that, in order of increasing S_c, the cycles to reach maximum weight gain C_m and the cycles to cross zero C_0 steadily decrease, whereas the terminal (negative) weight loss slope steadily increases. This result is the effect of altering only the scale (and spallation layers) to those with heavier metal (weight) contents with respect to the

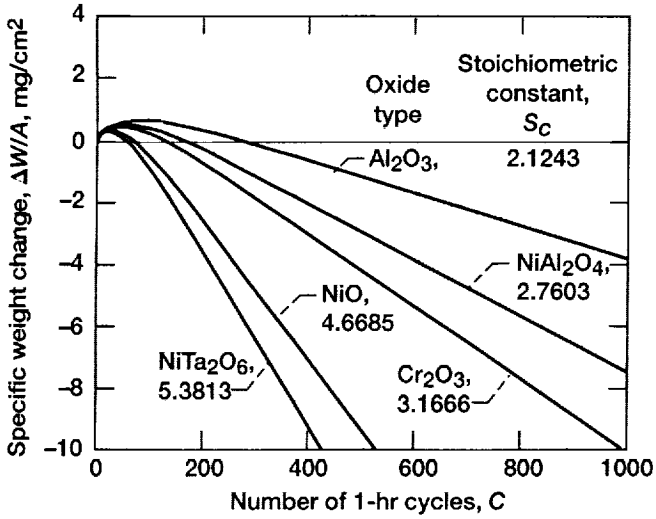

Figure 2.—Effect of oxide type (stoichiometric constant) on baseline COSP model curves for common (Ni-Cr-Al) oxides. Parabolic growth and uniform spalling case with parabolic rate constant k_p, 0.01 mg²/cm⁴hr; spall constant Q_0, 0.002 cm²/mg; and cycle duration Δt, 1 hr.

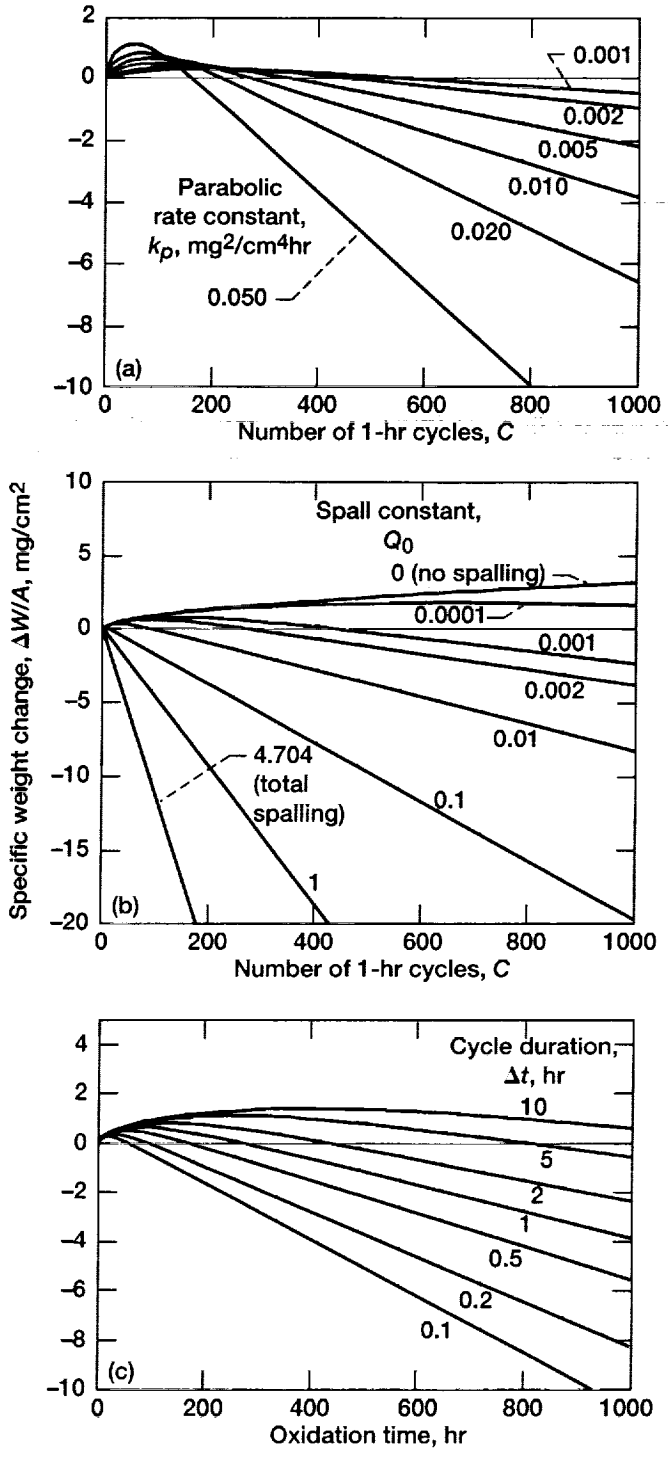

Figure 3.—Effect of parabolic rate constant, spall constant, and cycle duration on standard baseline COSP model curves for parabolic growth and uniform spalling of Al_2O_3 scale. Parabolic rate constant k_p, 0.01 mg²/cm⁴hr; spall constant Q_0, 0.002 cm²/mg; and cycle duration Δt = 1 hr. (a) k_p varied. (b) Q_0 varied. (c) Δt varied.

oxygen (weight) content. (The use of identical growth rates is unrealistic and is done here only for the sake of illustration.) Simple combined oxide stoichiometries can be used to represent multiple phases in the scale, such as $NiAl_2O_4$ to represent $NiO + Al_2O_3$. If a complex stoichiometry is needed and cannot be easily represented by a chemical formula, it is possible to enter any stoichiometric constant. For example, the arithmetic average of two constants may be entered to represent a scale consisting of a 50-50 percent mixture (by weight) of the two oxides.

Rate constant.—The effect of varying the rate constant k_p in the case of parabolic growth and uniform layer spallation, keeping Q_0 at 0.002 and cycle duration at 1 hr, is shown in figure 3(a) for an Al_2O_3 scale. Increasing k_p increases the maximum weight gain and the rate of final weight loss and decreases the cycles to both maximum and zero weight gain. The ratio C_m/C_0 remains essentially constant at 0.305 to 0.310.

Spall constant.—Figure 3(b) shows the effect of increasing the spall constant Q_0 for the case of parabolic growth and uniform layer spallation, fixing k_p at 0.01 mg^2/cm^4hr. Also shown for comparison are the two extremes of (a) zero spalling for Q_0 = 0.0 and (b) total spallation. For the case of total spallation in each cycle

$$F_s = 1.0 \tag{8}$$

From equation (4) one obtains

$$F_s = (Q_0)(W_r')^{\alpha} = 1.0 \tag{9}$$

and from equation (6)

$$W_r' = S_c(k_p \Delta t)^{1/2} \tag{6}$$

one derives that

$$Q_{0,\max} = \frac{1}{S_c(k_p \Delta t)^{1/2}} = 4.7074 \tag{10}$$

for this case of Al_2O_3. Between the two extremes, as Q_0 increases, the maximum weight gain steadily decreases, as does the number of cycles to maximum and zero weight gain. The ratio C_m/C_0 remains at about 0.31, where applicable. The final rate of weight loss increases with Q_0.

Cycle duration.—Finally, figure 3(c) shows the effect of cycle frequency (or duration). Here it is important to note whether the outputs are plotted versus cycle number or oxidation time. In this plot the maximum weight gain decreases with increasing cycle frequency, as do the number of hours to maximum and zero weight change. The ratio C_m/C_0 remains constant between 0.304 and 0.308. The final rate of weight loss increases with cycle frequency.

Growth law.—In most cases using a parabolic growth law is adequate for cyclic oxidation modeling. Deviations from parabolic kinetics are generally minor or require long oxidation times to become evident. Also, essentially parabolic curves can be fitted very nicely by adjusting both parameters (k and m) in the power growth law or logarithmic growth law models. This section illustrates some trends with growth parameters for these two other models. The baseline model is for Al_2O_3 with a spall constant Q_0 of 0.002 cm^2/mg and a cycle duration Δt of 1.0 hr.

Figure 4 shows the families of power growth law curves for varying k and m. In figure 4(a) increasing k for the cubic

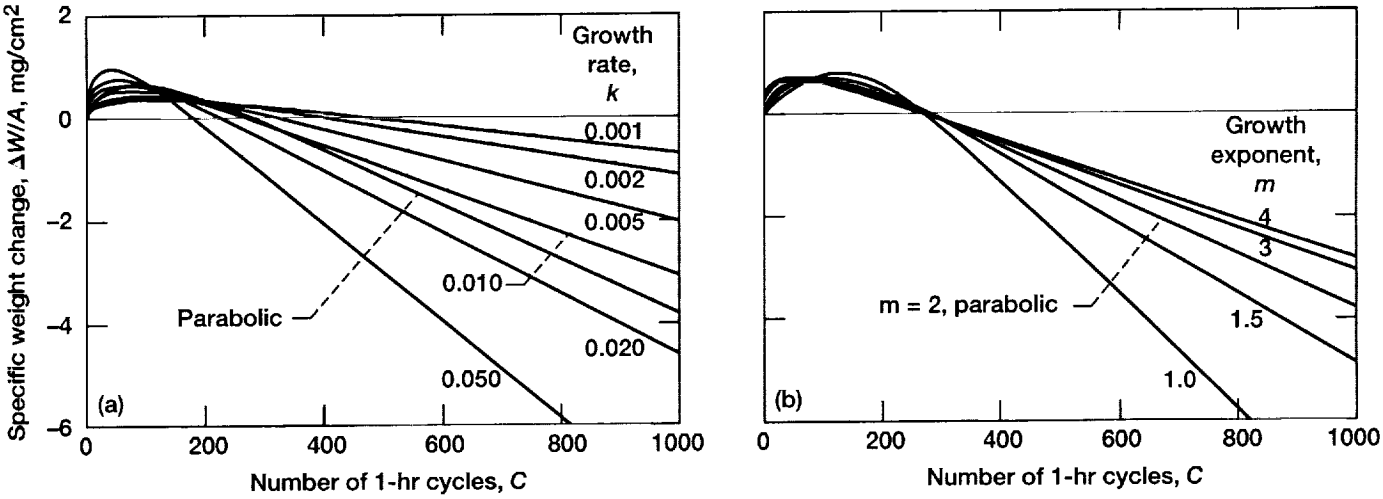

Figure 4.—Effect of power law growth kinetics on baseline COSP model curves for uniform spalling of Al_2O_3 scale. Spall constant Q_0, 0.002 cm^2/mg; cycle duration Δt, 1 hr. (a) Growth rate k varied for growth exponent m of 3. (b) m varied for k of 0.01.

(m = 3) case produces effects analogous to those shown in figure 3(a) for increasing k_p in parabolic growth. Again the ratio C_m/C_0 remains constant but now lies between 0.223 and 0.226.

In figure 4(b) subparabolic behavior ($m > 2$) lessens the final weight loss rate and shortens the time to reach maximum weight without appreciably shortening the time to reach zero weight change. Such models may be useful where fast-growing initial transient oxides give way to slower growing more stable scales or where oxide grain growth decreases the relative area of short-circuit pathways with time. Conversely, linear behavior (m = 1.0) lengthens the time to reach maximum weight and produces greater weight loss rates, as might be expected for a faster growing scale. The ratio C_m/C_0 is 0.47 for linear (m = 1), 0.30 for parabolic (m = 2), and 0.22 for cubic (m = 3) behavior.

Figure 5 shows families of logarithmic growth law curves for varying the rate constant k and the growth exponent m. In figure 5(a) the secondary growth constant c, which is the argument for the logarithm at t = 0, is set to 1.0 in order to yield zero-time weight change of 0.0. And m is set at 1.0 so that the weight change is simply given by ln ($kt + c$). The effects of increasing k are similar to those for the other two growth laws—increasing $(\Delta W/A)_{max}$ and increasing the final rate of weight loss. The ratio C_m/C_0 varies from 0.33 to 0.43 as k varies from 0.050 to 0.001 and is thus generally higher than the corresponding ratio for any parabolic case.

Figure 5(b) illustrates the effects of increasing m, with k fixed at 0.01. As in the power growth law case, increasing m reduces the final weight loss rate but now also produces a clear reduction in the maximum weight gain. Furthermore, the times to reach maximum or zero weight gain increase, with the ratio C_m/C_0 ranging from 0.40 (m = 0.5) to 0.33 (m = 4.0), again generally higher than the ratio (0.30) for any parabolic case.

It is generally true, then, that the power growth law and logarithmic growth law cases are more versatile in fitting a curve because of the additional adjustable parameters. However, this versatility implies a more complex process that becomes more difficult to confirm on the basis of established physical processes and well-known kinetics.

Spalling case.—Figure 6(a) compares the Monte Carlo, discrete segment, bimodal spalling distribution case against the uniform thickness spalling geometry. The same k_p (0.01), Q_0 (0.002), and Δt (1 hr) are used. Three bimodal models are shown for varying numbers of segments, each model with an R_{spall} of 1.0 (spalling to bare metal). At 10 segments one can see the wide diversions caused by sporadic spallation events, at 100 segments only noisy variations from monotonic behavior are seen, and at 1000 segments essentially a smooth curve is obtained with a very slight noise factor. The maximum weight gains are 0.62 mg/cm^2 for the bimodal case and 0.66 mg/cm^2 for the uniform spall model. These bimodal curves produce a final slope that is 40 percent larger than that for the uniform spalling case. However, the two spalling cases appear equivalent for the initial portion of the curve before reaching zero weight change.

Figure 6(b) shows the effect of varying R_{spall} from 0.1 to 1.0 for the same bimodal case with 1000 segments. At $R_{spall} \leq 0.1$ the bimodal case (line) is equivalent to uniform spalling (symbols) for this set of COSP conditions. Therefore, it is usually most practical to either use the uniform spall model case or the extreme bimodal case with R_{spall} = 1.0.

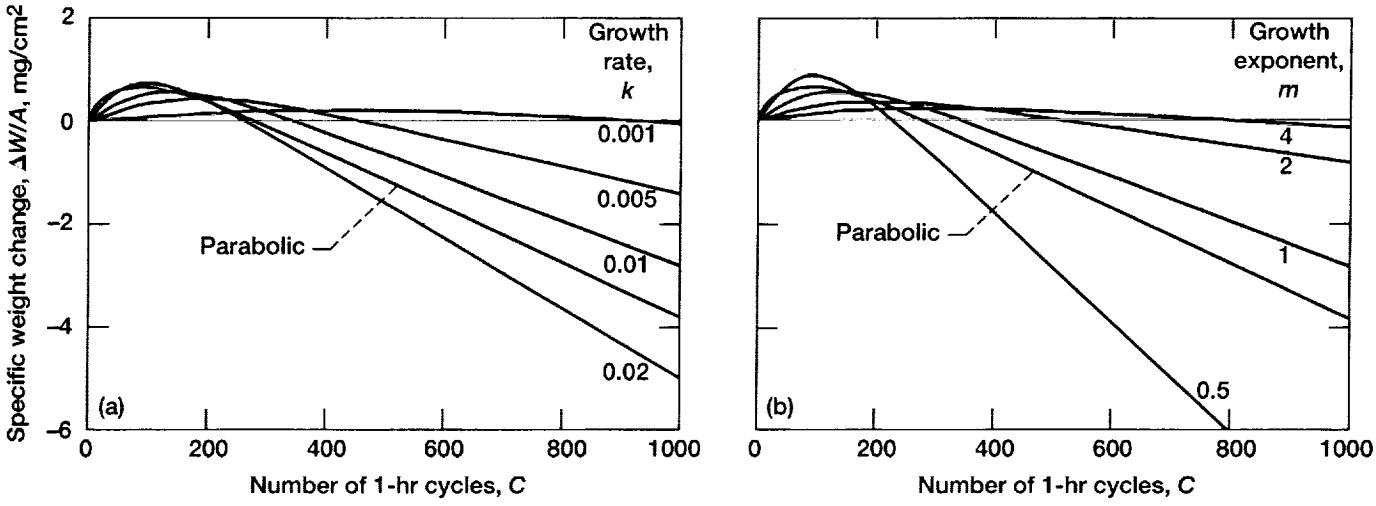

Figure 5.—Effect of logarithmic growth kinetics on baseline COSP model curves for uniform spalling of Al_2O_3 scale. Spall constant Q_0, 0.002 cm^2/mg; secondary growth constant c, 1; cycle duration Δt, 1 hr. (a) Growth rate k varied for growth exponent m of 1. (b) m varied for k of 0.01.

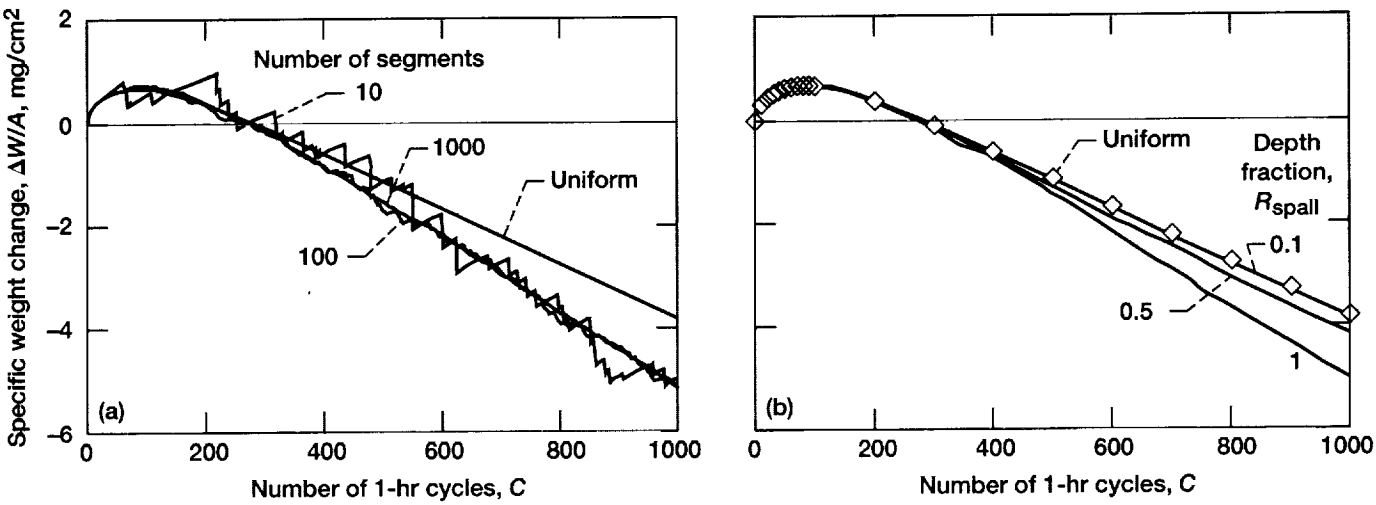

Figure 6.—Comparison of bimodal (Monte Carlo) spall model curves with uniform spalling case for baseline COSP model. Parabolic rate constant k_p, 0.01 mg^2/cm^{4}hr; spall constant Q_0, 0.002 cm^2/mg; and cycle duration Δt, 1 hr. (a) Serrated behavior for 10-segment surface and smooth behavior for ≥100-segment surface at depth fraction R_{spall} of 1.0. (b) Convergence to uniform spalling behavior for 1000-segment surface at $R_{spall} \leq 0.1$.

As originally stated in reference 7, the discrete bimodal spalling model is generally not needed for adequate modeling of a cyclic curve unless the spalling depth extends to bare metal ($R_{spall} = 1.0$). Therefore, it is most compelling to use the bimodal spalling case when it is well established that the spalling geometry is definitely interfacial in nature, as with poorly adherent scales, and not described by fracture at some level within the scale.

In summary, it has been well established that the characteristic parameters describing the model curves (C_m, C_0, C_m/C_0, $(\Delta W/A)_{max}$, and final slope) all vary in a regular mathematical fashion with the input parameters. These relationships have been previously analyzed by regression and presented in detail (ref. 7) and were recently summarized (ref. 8).

Basic Examples

Nickel Aluminides Plus Zirconium

Figure 7 shows experimental data obtained for the 1100 and 1200 °C cyclic oxidation of NiAl doped with 0.1 at.% zirconium (Zr) by Barrett (refs. 6 and 16). Also shown are COSP model curves obtained by iterative model selections for k_p and Q_0, assuming the parabolic growth law and the uniform spalling case. At 1100 and 1200 °C the corresponding values of k_p were 0.0025 and 0.0170 mg^2/cm^{4}hr, respectively, and the values of Q_0 were extremely low, 0.00002 and 0.000095 cm^2/mg, respectively. These two very well behaved, long-time curves lend themselves to excellent fits by the COSP model.

The corresponding k_p value was determined from 100-hr isothermal tests of the same alloy at 1200 °C to be 0.0276 mg^2/cm^{4}hr, or nearly 50 percent higher than those predicted by the model. In isothermal tests of similar NiAl + Zr alloys the 1100 and 1200 °C rate constants were 0.00132 and 0.00553 mg^2/cm^{4}hr, respectively, or more than 50 percent less than those predicted by the model (ref. 17). For low oxidation rates this degree of variability is not especially uncommon. Although the agreement with independent isothermal tests is within an order of magnitude, it is not necessarily precise. The physical process (parabolic growth) may somehow be indirectly modified by the very action of cycling, but it is not clear how this would happen.

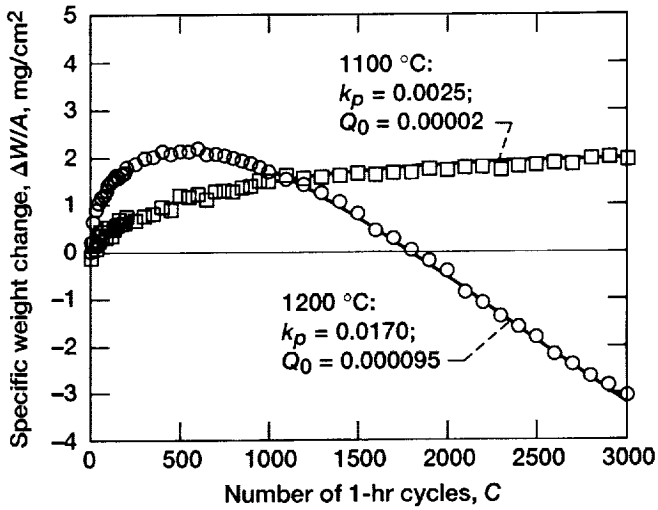

Figure 7.—COSP model (curves) for fitted parabolic growth and uniform spall case with 1100 and 1200 °C cyclic oxidation data (symbols) for NiAl + 0.1 Zr using 1-hr cycles (refs. 6 and 16).

We suggest that some nonideality in the spalling sequence (unpredictable variations in Q_0) may produce a skewed fit and give the appearance of a different growth constant. Although it is straightforward to independently confirm the parabolic growth kinetics in isothermal thermogravimetric tests, it is much more difficult to establish the true extent and geometry of the spalling process over a large number of cycles (ref. 2). Thus, some caution is appropriate regarding the degree of comparability between cyclic modeling and isothermal tests.

Single-Crystal Superalloys

Samples of PWA 1480 were prepared and hydrogen annealed (desulfurized) to various sulfur levels in order to produce different levels of scale adhesion in 1100 °C cyclic tests (ref. 18). Figure 8 shows that at low sulfur (S) levels (≤0.2 ppmw) excellent scale adhesion was produced and minimal spalling occurred over the 1000 1-hr cycle tests (sample 20–6, H_2 annealed for 100 hr at 1200 °C to 0.14 ppmw S). Here it is immediately established that even the best fit to a parabolic model, with $k_p = 1.2\times10^{-3}$ mg^2/cm^{4}hr and $C_m/C_0 = 0.31$, cannot adequately follow the shape of the actual curve. However, a power growth law model, with $m = 4$ and $k = 0.00075$, produces $C_m/C_0 = 0.18$ and fits the data exceptionally well. This model calculates the fraction of scale spalled to be 0.075 percent and the retained scale weight to be 1.49 mg/cm^2 after 1000 cycles. The improved fit of the power law model versus the parabolic growth model is due to the initial period (20 hr) of strong transient oxidation.

Although it is generally assumed that the protective behavior of single-crystal superalloys is derived from parabolic growth of α-Al_2O_3, it is also known that the initial transient growth of $NiAl_2O_4$ is relatively large (ref. 19), giving the appearance of nonparabolic growth. Independent 1100 °C isothermal tests have identified deviations from parabolic growth for approximately the first 16 hr of oxidation, producing essentially a 0.11-mg/cm^2 transient oxidation "y intercept" on a $t^{1/2}$ parabolic plot (ref. 20). The parabolic kinetics were described by a k_p of 6.5×10^{-4} mg^2/cm^{4}hr in contrast to 1.2×10^{-3} mg^2/cm^{4}hr in the parabolic fit here. Both parabolic and power growth law COSP models yield spall constants Q_0 very close to 0.0005 cm^2/mg, which is a relatively small factor owing to the strong scale adhesion observed in the low-sulfur samples.

At a slightly higher sulfur level (sample 20–5, H_2 annealed for 8 hr at 1200 °C to 0.8 ppmw S), more spalling took place and negative weight changes were sustained. Figure 9 shows the experimental data along with three model curves. The power growth law model used the same growth parameters as determined in figure 8 for the more adherent scale. The parabolic model was best fit by a k_p of 5×10^{-3} mg^2/cm^{4}hr. The spalling constants were 0.010 to 0.015 cm^2/mg, or ≥20 times the constants determined for the low-sulfur sample in figure 8. Some deviation from a good fit is apparent for the longer test times. Here the bimodal case, with $R_{spall} = 1.0$ for bare-metal spalling, shows perhaps the best overall agreement as Al_2O_3 interfacial spallation becomes a more prominent feature of the cyclic oxidation process (now with $F_s = 1.2$ percent, in contrast to 0.075 percent for sample 20–6 with 0.14 ppm S at the end of 1000 cycles). The calculated weight of the scale retained after 1000 cycles is 0.93 mg/cm^2.

Figure 10 illustrates even higher sulfur samples (sample 50–3, H_2 annealed for 20 hr at 1200 °C to 1.5 ppmw S; and sample 20–0, with 6.7 ppmw S, not annealed). Using the same power law growth parameters for Al_2O_3 scales, the values of Q_0 were now determined to be at the higher levels of 0.05 and 0.5 cm^2/mg, respectively. However, these fits were not adequate, especially at the longer times. X-ray diffraction identified nickel tantalate ($NiTa_2O_6$, or an equivalent rutile structure) as the major scale phase owing to massive spallation, aluminum depletion, and a shift in oxide type from predominantly α-Al_2O_3 scales to

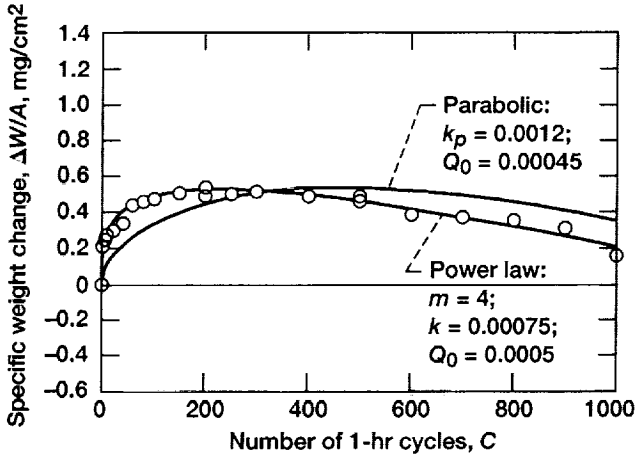

Figure 8.—COSP model power law fit to 1100 °C cyclic oxidation behavior of PWA 1480 using 1-hr cycles; H_2 annealed to 0.14 ppmw S (ref. 17).

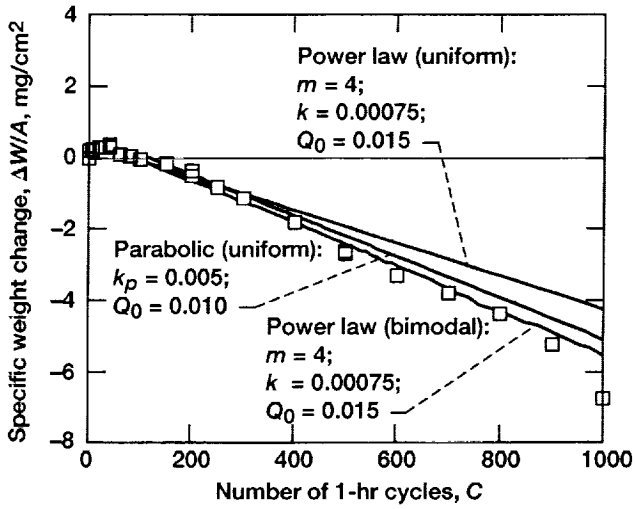

Figure 9.—COSP power law growth and bimodal spalling model fit to 1100 °C cyclic oxidation behavior of PWA 1480 using 1-hr cycles; H_2 annealed to 0.8 ppmw S (ref. 17).

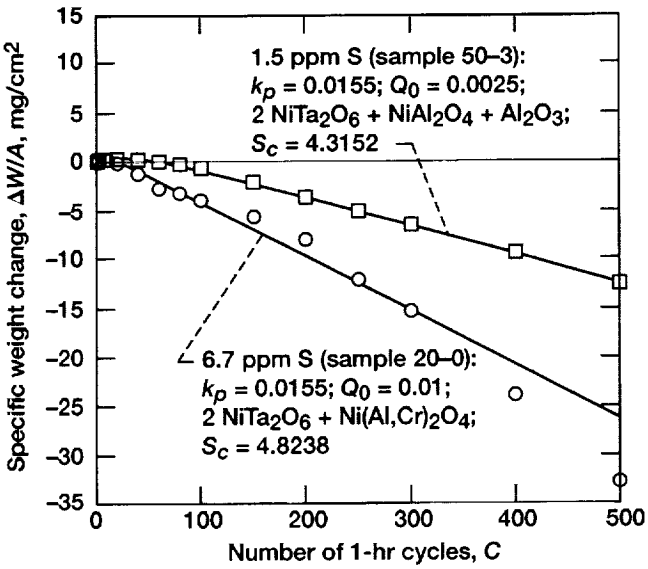

Figure 10.—COSP model fit to 1100 °C cyclic oxidation behavior of PWA 1480 using 1-hr cycles; H_2 annealed to 1.5 ppmw S or 6.7 ppmw S for no annealing (ref. 17). (Curves denote model predictions; symbols denote experimental data.)

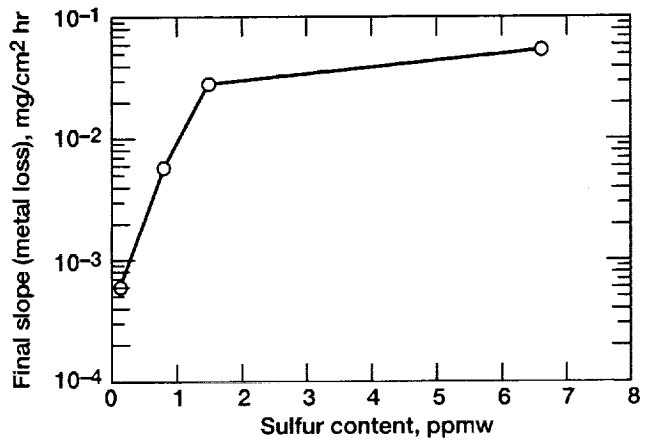

Figure 11.—Metal consumption rates during cyclic oxidation of PWA 1480 as function of alloy bulk sulfur content.

heavier Ni,Ta scales. Thus, for sample 50–3, with 1.5 ppmw S, an estimated stoichiometric constant (from twice as much rutile as spinel plus alumina) of 4.3152 is derived, and an excellent fit is obtained by a parabolic COSP model. Parabolic fits employ heavier nonprotective oxides owing to excessive initial interfacial spalling. Similarly, for sample 20–0, at 6.7 ppmw S, the diffraction data suggest a major rutile phase with lesser amounts of a mixed spinel, yielding a stoichiometric constant of 4.8238. (By comparison, S_c = 5.3813 for pure $NiTa_2O_6$). However, the multiple inflections in these data indicate numerous mechanism changes that prevent a fit by just one model. The calculated fraction of oxide spalled and the final retained scale weight

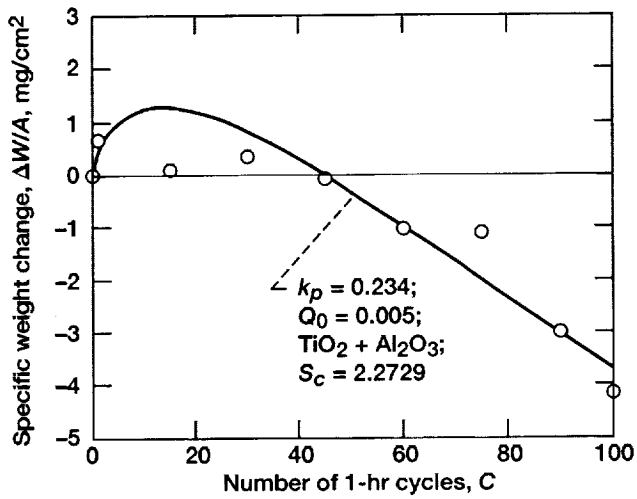

Figure 12.—Rough model fit, using mixed oxide stoichiometry and relatively high growth constant, to erratic behavior of Ti-24Al-11Nb (at.%) in 982 °C cyclic oxidation with 1-hr cycles. (Curve denotes model prediction; symbols denote experimental data.)

were 0.97 percent and 3.83 mg/cm², respectively, for sample 50–3 and 2.63 percent and 2.56 mg/cm² for sample 20–0.

The effect of sulfur content on weight change behavior can be connected to various model parameters. Initially, Q_0 would seem to be the logical figure of merit. However, because of changes in the oxide phase and the growth models above 1 ppmw sulfur, a simple relationship was not found. Instead, the final slope of the model curves was examined, as this is equivalent to the rate of metal consumed and represents the ultimate measure of material wastage. The results plotted in figure 11 indicate a relatively smooth curve. An increase of two orders of magnitude in metal consumption rate occurs between 0 and 10 ppmw sulfur, with most of the effect between 0 and 2 ppmw.

Rather than depend only on the weight change data for these mechanistic transitions, it would also be advisable to use models of solute depletion and diffusion modeling to define a critical flux required to sustain protective scale formation. Such a computer model has been developed (COSIM) and coupled with COSP to account for these transitions to less protective behavior (ref. 21).

Titanium Aluminides

Another nonprotective system, with a considerable amount of fast-growing titanium dioxide (TiO_2) making up the scale, is now considered. High-temperature structural titanium aluminides have been engineered with excellent specific strength at intermediate temperatures, but they suffer from rapid oxidation kinetics at high temperatures. Figure 12 (ref. 22) shows the 982 °C cyclic oxidation data for one such alloy, α_2-Ti_3Al + Nb (24Al-11Nb in at.%). Considerable weight loss has been

sustained after only 100 1-hr cycles of testing. The data are rather erratic, so that no single model can provide a satisfactory fit. However, the average behavior has been approximated by a model using a 50-50 molar mix of TiO_2-Al_2O_3, a k_p of 0.234 mg^2/cm^4hr (obtained from independent isothermal tests of similar alloys, ref. 23), and a Q_0 of 0.005. By assuming an oxide stoichiometry of either pure TiO_2 or pure Al_2O_3, essentially the same oxidation curve was maintained, with corresponding Q_0 of either 0.0035 or 0.0065, respectively. The point is that information can be obtained for nonprotective complex scales with some consistency from independent tests. However, the danger always remains that the counteradjustment of two parameters may produce a reasonable fit that may not be firmly justified by these tests.

Model Restrictions

Certain combinations of input variables may preclude a physically meaningful or mathematically logical calculation of the oxidation curve:

1. **The spall constant input Q_0 shall not be so high as to produce a spall fraction F_s greater than unity.** The fraction spalled F_s of the existing scale weight W_r' is given by $F_s = Q_0 (W_r')^{\alpha}$. Therefore, as W_r' increases with time (as governed by k_p), F_s also increases. It is then quite possible that before the limiting oxide weight is achieved according to COSP, the quantity $Q_0 (W_r')^{\alpha}$ will exceed unity, a physical impossibility. At this juncture the calculations are halted and a warning message is triggered, recommending that a lower value of Q_0 be tried.
2. **In Monte Carlo cases the input value of R_{spall} shall not be so low as to cause the spall fraction F_s to be less than that dictated by Q_0.** In the present version of COSP the bimodal case of nonuniform, random (Monte Carlo) spalling of individual segments is defined by the average spall fraction F_{avg} as given by $F_{avg} = PR_{spall}$, where P and R_{spall} are the probability and specified depth fraction of spalling. If R_{spall} is set too low, then even with $P = 1.0$ (the maximum probability), F_{avg} determined from $F_{avg} = PR_{spall}$ may still be less than that required by $F_{avg} = Q_0 (W_r')^{\alpha}$. If this condition occurs, calculations are halted and a warning message will be triggered, recommending that a larger value of R_{spall} be tried. (Conversely, a smaller value of Q_0 may also remedy this inconsistency.)
3. **Multiplicity/ambiguity of input parameters may occur in fitting experimental curves.** This restriction is a general warning that various combinations of input parameters may, especially in extreme cases, provide seemingly equally acceptable fits to a desired cyclic oxidation curve, but with unacceptable physical basis in reality. For example, a strongly negative slope in weight change may be provided by the product of many combinations of k_p and Q_0. However, only a restricted range of k_p is realistic for a given oxide type at a given temperature. Typical values may be provided from the literature or from independent tests. It is generally advisable to perform sensitivity tests on the effect of input parameters on the various descriptive parameters. The specific relationship of the descriptive parameters to the various combinations of input parameters indicates which factors will produce these equivalent multiplicity effects (ref. 7).

Concluding Remarks

The preceding text has provided a tour through the major operating features of COSP for Windows (WinCOSP), a Windows-based computer program developed to reproduce and model the cyclic oxidation weight change behavior of metals and alloys. Model curves have been presented to show the major trends in weight change, scale growth, spallation, and material consumption with variations of input parameters for a number of growth and spalling cases. For a single well-behaved cyclic curve it is especially useful to be able to extract parameters such as the rate constant, the scale thickness, the fraction of oxide spalled, and the total amount of metal consumed.

Examples have been presented to illustrate classic monotonic behavior and good agreement, such as for NiAl + Zr. Also, nonparabolic (logarithmic) cases with large transients and deviation from a single spalling model have been proposed for the superalloy PWA 1480. A major discontinuity was observed for the higher sulfur contents, with the eventual change from primarily Al_2O_3 to Ni,Ta-rich oxides. Here the use of a higher stoichiometric constant markedly improved the model fit to the data. Despite these specific idiosyncrasies, the overall modeling effort was informative in determining metal consumption rates as a function of sulfur content.

A number of concerns exist regarding overselling the agreement of any specific model with a set of experimental data. There is never any guarantee that good agreement with one model automatically precludes equally good agreement with some other model. Furthermore, agreement with 1000-hr data does not necessarily guarantee unqualified predictive ability for 10 000-hr data. It is strongly recommended that model parameters be critically evaluated by independent measures of oxide type, scale growth, and spalling modes. The models should be presented as reasonable fits to the data for the purpose of showing major trends and consistent near-term predictions, but should not be claimed as categorical proof of detailed mechanisms for indefinite exposure times.

COSP for Windows can be obtained for individual use by contacting the authors, James.L.Smialek@grc.nasa.gov or Judith.V.Auping@grc.nasa.gov.

Glenn Research Center
National Aeronautics and Space Administration
Cleveland, Ohio, November 2001

References

1. Barrett, C.A.; and Pressler, A.F.: COREST: A Fortran Computer Program to Analyze Paralinear Oxidation Behavior and its Application to Chromic Oxide Forming Alloys. NASA TN D–8132, 1976.
2. Smialek, J.L.: Oxide Morphology and Spalling Model for NiAl. Metall. Trans., vol. 9A, 1978, pp. 309–320.
3. Barrett, C.A.; and Lowell, C.E.: High Temperature Cyclic Oxidation Furnace Testing at NASA Lewis Research Center. NASA TM–81773, 1981.
4. Lowell, C.E.; Smialek, J.L.; and Barrett, C.A.: Cyclic Oxidation of Superalloys. High Temperature Corrosion, NACE 6, R.A. Rapp, ed., 1983, pp. 219–226.
5. Probst, H.B.; and Lowell, C.E.: Computer Simulation of Cyclic Oxidation. J. Met., vol. 40, no. 10, 1988, pp. 18–21.
6. Barrett, C.A.: The Effect of 0.1 Atomic Percent Zirconium on the Cyclic Oxidation Behavior of β-NiAl for 3000 Hours at 1200 °C. Proceedings of the Workshop on the Oxidation of High Temperature Intermetallics, T. Grobstein and J. Doychak, eds., TMS, Warrendale, PA, 1988, pp. 67–82.
7. Lowell, C.E.; et al.: COSP: A Computer Model of Cyclic Oxidation. Oxid. Met., vol. 36, nos. 1/2, 1991, pp. 81–112.
8. Smialek, J.L.; et al.: Cyclic Oxidation Testing and Modeling: A NASA Lewis Perspective. Cyclic Oxidation of High Temperature Materials, M. Schutze and W.J. Quadakkers, eds., European Federation of Corrosion, Institute of Materials, London, 1999, pp. 148–168. (Also NASA/TM—2000-209769, 2000.)
9. Barrett, C.A.: 10 000 Hour Cyclic Oxidation Behavior at 815 °C (1500 °F) of 33 High-Temperature Alloys. Environmental Degradation of Materials, Virginia Polytechnic Institute, Blacksburg, VA, 1977, pp. 319–327.
10. Barrett, C.A.; and Lowell, C.E.: High Temperature Cyclic Oxidation Furnace Testing at NASA Lewis Research Center. JTEVA, vol. 10, no. 6, 1982, pp. 273–278. (Also NASA TM–81773, 1981.)
11. Smialek, J.L.; and Meier, G.H.: High-Temperature Oxidation. Chapter 11 in Superalloys II, C.T. Sims, N.S. Stoloff, and W.C. Hagel, eds., Wiley, New York, 1987, pp. 293–326.
12. Barrett, C.A.; Garlick, R.G.; and Lowell, C.E.: High-Temperature Cyclic Oxidation Data, pt. 1, NASA TM–83665, 1984.
13. Barrett, C.A.; and Garlick, R.G.: High-Temperature Cyclic Oxidation Data, pt. 2, NASA TM–101468, 1989.
14. Smialek, J.L.; Barrett, C.A.; and Schaeffer, J.C.: Design for Oxidation Resistance. ASM Handbook, Vol. 20, Materials Selection and Design, ASM International, Materials Park, OH, 1997, pp. 589–602.
15. Barrett, C.A.: 10 000-Hour Cyclic Oxidation Behavior at 982 °C (1800 °F) of 68 High-Temperature Co-, Fe-, and Ni-Base Alloys. NASA TM–107394, 1997.
16. Barrett, C.A.: Effect of 0.1% Zr on the Cyclic Oxidation Behavior of β-NiAl. Oxid. Met., vol. 30, nos. 5/6, 1988, pp. 361–390.
17. Rybicki, G.C.; and Smialek, J.L.: Effect of the θ- to α-Al_2O_3 Transformation on the Oxidation Behavior of β-NiAl + Zr. Oxid. Met., vol. 31, 1989, pp. 275–304.
18. Smialek, J.L.: Toward Optimum Scale and TBC Adhesion on Single Crystal Superalloys. High Temperature Corrosion and Materials Chemistry, P.Y. Hou, et al., eds., The Electrochemical Society Proceedings, Vol. 98–9, Pennington, NJ, 1998, pp. 211–220.
19. Pint, B.A.; Tortorelli, P.F.; and Wright, I.G.: Effect of Cycle Frequency on High Temperature Oxidation Behavior of Alumina- and Chromia-Forming Alloys. Cyclic Oxidation of High Temperature Materials, M. Schutze and W.J. Quadakkers, eds., European Federation of Corrosion, Institute of Materials, London, 1999, pp. 111–132.
20. McVay, R; and Williams, P.: The Effect of Low Sulfur and Oxygen Active Elements on the Oxidation Resistance of Single Crystal Superalloys. Senior Thesis, U. of Pittsburgh, G. Meier and F. Pettit, advisors, Pittsburgh, PA, 1992.
21. Nesbitt, J.A.: Diffusional Aspects of the High Temperature Oxidation of Protective Coatings. Diffusion Analysis and Applications, A.D. Romig and M.A. Dayanada, eds., TMS, Warrendale, PA, 1989, pp. 307–324.
22. Smialek, J.L.; Gedwill, M.A.; and Brindley, P.K.: Cyclic Oxidation of Aluminide Coatings on Ti_3Al + Nb. Scripta Met. et Mat., vol. 24, 1990, pp. 1291–1296.
23. Wiedemann, K.E.; et al.: Static and Dynamic Oxidation of Ti-14Al-21Nb. Oxidation of High-Temperature Intermetallics, T. Grobstein and J. Doychak, eds., TMS, Warrendale, PA, 1988, pp. 195–206.

REPORT DOCUMENTATION PAGE

Form Approved
OMB No. 0704-0188

1. AGENCY USE ONLY (*Leave blank*)	2. REPORT DATE	3. REPORT TYPE AND DATES COVERED
	February 2002	Technical Paper

4. TITLE AND SUBTITLE

COSP for Windows: Strategies for Rapid Analyses of Cyclic Oxidation Behavior

5. FUNDING NUMBERS

WU–708–31–13–00

6. AUTHOR(S)

James L. Smialek and Judith V. Auping

7. PERFORMING ORGANIZATION NAME(S) AND ADDRESS(ES)

National Aeronautics and Space Administration
John H. Glenn Research Center at Lewis Field
Cleveland, Ohio 44135–3191

8. PERFORMING ORGANIZATION REPORT NUMBER

E–12955

9. SPONSORING/MONITORING AGENCY NAME(S) AND ADDRESS(ES)

National Aeronautics and Space Administration
Washington, DC 20546–0001

10. SPONSORING/MONITORING AGENCY REPORT NUMBER

NASA TP—2002-211108

11. SUPPLEMENTARY NOTES

Responsible person, James L. Smialek, organization code 5160, 216–433–5500.

12a. DISTRIBUTION/AVAILABILITY STATEMENT

Unclassified - Unlimited
Subject Category: 26 Distribution: Standard

Available electronically at http://gltrs.grc.nasa.gov/GLTRS

This publication is available from the NASA Center for AeroSpace Information, 301–621–0390.

12b. DISTRIBUTION CODE

13. ABSTRACT ***(Maximum 200 words)***

COSP is a publicly available computer program that models the cyclic oxidation weight gain and spallation process. Inputs to the model include the selection of an oxidation growth law and a spalling geometry, plus oxide phase, growth rate, spall constant, and cycle duration parameters. Output includes weight change, the amounts of retained and spalled oxide, the total oxygen and metal consumed, and the terminal rates of weight loss and metal consumption. The present version is Windows based and can accordingly be operated conveniently while other applications remain open for importing experimental weight change data, storing model output data, or plotting model curves. Point-and-click operating features include multiple drop-down menus for input parameters, data importing, and quick, on-screen plots showing one selection of the six output parameters for up to 10 models. A run summary text lists various characteristic parameters that are helpful in describing cyclic behavior, such as the maximum weight change, the number of cycles to reach the maximum weight gain or zero weight change, the ratio of these, and the final rate of weight loss. The program includes save and print options as well as a help file. Families of model curves readily show the sensitivity to various input parameters. The cyclic behaviors of nickel aluminide (NiAl) and a complex superalloy are shown to be properly fitted by model curves. However, caution is always advised regarding the uniqueness claimed for any specific set of input parameters.

14. SUBJECT TERMS

Cyclic oxidation; Weight change curves; Growth kinetics; Spalling; Computer models

15. NUMBER OF PAGES

17

16. PRICE CODE

17. SECURITY CLASSIFICATION OF REPORT	18. SECURITY CLASSIFICATION OF THIS PAGE	19. SECURITY CLASSIFICATION OF ABSTRACT	20. LIMITATION OF ABSTRACT
Unclassified	Unclassified	Unclassified	